

Shape and stability of doubly connected axisymmetric free surfaces in a cylindrical container

Lev A. Slobozhanin,^{a)} J. Iwan D. Alexander, and Alexandre I. Fedoseyev^{a)}
*Department of Mechanical and Aerospace Engineering and National Center for Microgravity,
 Research on Fluids and Combustion, Case Western Reserve University, Cleveland, Ohio 44106*

(Received 11 June 1999; accepted 18 August 1999)

The equilibrium and stability of a liquid that partially fills a cylindrical container with planar ends are examined. It is assumed that the free surface is axisymmetric and does not cross the symmetry axis of the container. Particular attention is given to the case where gravity is parallel to the cylinder's axis, and where the free surface has one contact line on the lateral cylindrical wall and the other on one of the planar ends. The equilibrium configuration of such a surface is determined by the wetting angle, α , the Bond number, B , and the relative volume, V , of the annular region bounded by the free surface and the solid container. Shapes of stable and critical surfaces have been analyzed, and the stability regions for arbitrary Bond numbers have been obtained in the α - V plane. The shape and stability problems for a zero gravity configuration with both contact lines on the lateral wall of the cylinder are also studied. In addition, the stability of a free surface with at least one contact line coinciding with the edge formed by the lateral wall and a planar end is discussed.

© 1999 American Institute of Physics. [S1070-6631(99)00812-0]

I. INTRODUCTION

This paper concerns the shape and stability of axisymmetric equilibrium configurations of a liquid that partially fills a circular cylindrical container with flat ends orthogonal to the cylinder's axis. Either the liquid is subject to a steady axial acceleration field or zero gravity conditions are assumed to prevail. The free surface is assumed to be connected i.e., it consists of one piece. The shape and stability of simply connected axisymmetric surfaces (i.e., the surface crosses the cylinder's axis of symmetry) have already been studied. The stability of a simply connected surface in contact with a smooth cylinder wall has been analyzed by Tyuptsov¹ (see also Ref. 2). The stability problem for a simply connected free surface in contact with a smooth flat endwall is identical to the stability problem for a bubble (or a drop) on a horizontal plane. This classical problem has inspired many publications (see, for example, Myshkis *et al.*,² Michael,³ and Finn⁴ for results and references).

Here we consider the shape and stability problems for *doubly connected* free surfaces. A doubly connected axisymmetric surface is an annular surface. That is, it does not cross the cylinder's symmetry axis. Until now, doubly connected surfaces have only been studied for cases where the free surface has contact lines on different flat ends of the container. This case is identical to a liquid bridge between horizontal parallel plates (see Refs. 2 and 5–10). However, like the above-mentioned case of a bubble (or a drop) on a horizontal plane, it does not account for the effect of the geometrical properties peculiar to a cylindrical container. Thus, there is a need to study problems where the shape and sta-

bility of the configuration are influenced by the existence of a cylindrical wall. Our investigation is motivated by basic scientific interest and practical considerations (since cylindrical vessels are commonly used containers). Furthermore, the selection of the configurations we examined was also guided by the possibility of melt detachment from the container wall during directional solidification by the Bridgman method under low gravity conditions.¹¹

First, we focus attention on free surfaces with contact lines located on smooth solid surfaces. These are free surfaces with one of the contact lines on a flat endwall and the other on a lateral wall, and free surfaces with both contact lines on a lateral wall. It is assumed that the container material is homogeneous and, thus, the wetting angle α is constant over the entire solid surface. (Annular free surfaces with both contact lines on one of the cylinder's flat ends cannot exist under this assumption.) Then we analyze cases where at least one of the contact lines coincides with the edge formed by the cylindrical wall and one of the flat ends.

It is assumed that the annular region between the walls of the cylindrical container and the free surface is occupied by a gas. With the help of duality concepts (see Ref. 2), the treatment of such a liquid-gas system can be extended directly to a system for which the relative positions of the gas and the liquid are reversed. This is achieved by replacing the wetting angle α with the supplementary angle $180^\circ - \alpha$. To account for the reversal in sign of the density difference that results when changing the gas-liquid positions the orientation of the gravity vector must be reversed.

Aside from the wetting angle α , the system under consideration is characterized by relative volume of the gas, V , and the Bond number, B . They are given by

$$V = \nu/r_0^3, \quad B = \rho g r_0^2 / \sigma. \quad (1)$$

^{a)}Center for Microgravity and Materials Research, University of Alabama in Huntsville, Huntsville, Alabama 35899.

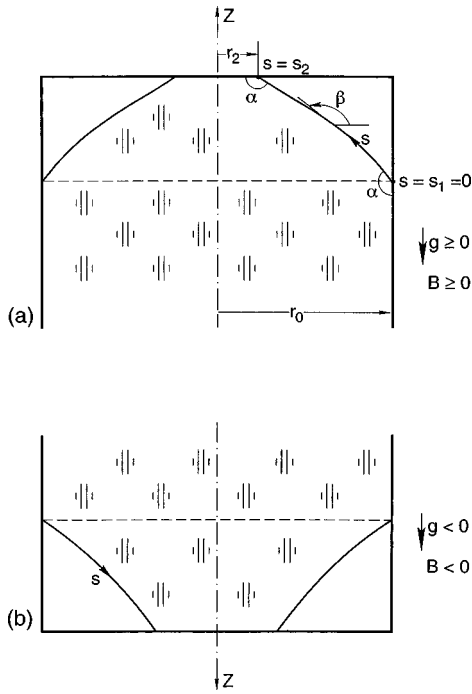


FIG. 1. Equilibrium configuration with an annular free surface in contact with a cylindrical wall and a flat endwall, (a) $B > 0$; (b) $B < 0$.

Here, ν is the actual gas volume, r_0 is the cylinder radius, g is the gravity acceleration, and ρ and σ are the liquid density and surface tension, respectively. We assume that gravity acts down and along the z -axis of a cylindrical coordinate system. We take $g > 0$ ($B > 0$) if the gas cavity is at the top of the cylinder, and $g < 0$ ($B < 0$) if the gas cavity is at the bottom (see Fig. 1).

The problem is formulated in Sec. II, and the results for free surfaces in contact with smooth solid surfaces are described in Secs. III A and III B. In Sec. III C it is shown that other types of doubly connected equilibrium free surfaces do not exist if the wetting angle α is constant over the entire container. These surfaces are annular surfaces that have both contact lines on one of the flat endwalls, or free surfaces with at least one contact line located on the edge formed by the cylinder wall and one endwall. The stability conditions for the latter are discussed for the case when the wetting angles on the lateral wall and on a flat end are different.

II. FORMULATION

A. Equilibrium free surfaces

The axisymmetric equilibrium surface has a parametric representation $r(s)$ and $z(s)$, where r , θ , and z are cylindrical coordinates, and s is the arc length of a surface axial section $\theta = \text{const}$ (see Fig. 1). This section determines the surface equilibrium profile. The functions $r(s)$ and $z(s)$ are the solutions of the ordinary differential equations:²

$$r'' = -z' \beta', \quad z'' = r' \beta', \quad \beta' = -bz + q - \frac{z'}{r},$$

$$\left(s_1 \leq s \leq s_2, \quad ' = \frac{d}{ds} \right). \tag{2}$$

Here, $b = \rho g / \sigma$, q is twice the mean curvature of the surface at $z = 0$, and $\beta = \beta(s)$ is the angle measured from the r axis to the tangent to the equilibrium profile directed in the sense of increasing s . It is assumed that the domain occupied by the liquid remains to the left as one moves along the profile in the direction of increasing s . The endpoints $r(s_1)$, $z(s_1)$ and $r(s_2)$, $z(s_2)$ must belong to the axial section of a cylindrical container. Furthermore, if the contact lines lie on smooth solid surfaces, the slope (with respect to the solid walls) of the equilibrium profile at the endpoints must correspond to the tangent of the given wetting angle α . The quantity q is determined by the condition that the annular region bounded by the equilibrium surface and the container has a given gas volume.

B. Stability of doubly connected axisymmetric equilibrium surfaces

According to Ref. 2, the stability problem for doubly connected axisymmetric free surfaces in contact with smooth surfaces of a cylindrical container is reduced to determination of the sign of the smallest eigenvalue λ_{01} for the problem

$$L\varphi_0 + \mu = \lambda \varphi_0 \quad (s_1 \leq s \leq s_2), \tag{3}$$

$$-\varphi_0'(s_1) + \chi_1 \varphi_0(s_1) = 0, \quad \varphi_0'(s_2) + \chi_2 \varphi_0(s_2) = 0, \tag{4}$$

$$\int_{s_1}^{s_2} r \varphi_0 ds = 0, \tag{5}$$

and of the sign of the smallest eigenvalue λ_{11} for the problem

$$L\varphi_1 + \frac{1}{r^2} \varphi_1 = \lambda \varphi_1 \quad (s_1 \leq s \leq s_2), \tag{6}$$

$$-\varphi_1'(s_1) + \chi_1 \varphi_1(s_1) = 0, \quad \varphi_1'(s_2) + \chi_2 \varphi_1(s_2) = 0. \tag{7}$$

Here,

$$L\varphi \equiv -\varphi'' - \frac{r'}{r} \varphi' + a(s)\varphi, \tag{8}$$

$$a(s) = -br' - \beta'^2 - \frac{z'^2}{r^2}, \tag{9}$$

$$\chi_1 = -\beta'(s_1) \cot \alpha, \quad \chi_2 = -\beta'(s_2) \cot \alpha; \tag{10}$$

μ is an unknown constant, and $\varphi_0 = \varphi_0(s)$, $\varphi_1 = \varphi_1(s)$. The equilibrium is stable (unstable) to axisymmetric perturbations if $\lambda_{01} > 0$ ($\lambda_{01} < 0$), and is stable (unstable) to nonaxisymmetric perturbations if $\lambda_{11} > 0$ ($\lambda_{11} < 0$). The equilibrium is stable (to arbitrary perturbations) if $\lambda^* = \min(\lambda_{01}, \lambda_{11}) > 0$. The equilibrium is neutrally stable to axisymmetric (nonaxisymmetric) perturbations if $\lambda_{01} = 0$ ($\lambda_{11} = 0$). Finally, the equilibrium state is critical to axisymmetric perturbations if $0 = \lambda_{01} < \lambda_{11}$, and is critical to nonaxisymmetric perturbations if $0 = \lambda_{11} < \lambda_{01}$.

The conditions that an eigenvalue of the problem (3)–(5) or problem (6)–(7) is equal to zero are, respectively, of the form

$$D_0 \equiv \det \left(\begin{array}{c} -u'_{0i}(s_1) + \chi_1 u_{0i}(s_1), \quad u'_{0i}(s_2) + \chi_2 u_{0i}(s_2), \\ \int_{s_1}^{s_2} r u_{0i} ds \end{array} \right)_{i=1,2,3} = 0, \quad (11)$$

$$D_1 \equiv \det(-u'_{1i}(s_1) + \chi_1 u_{1i}(s_1), \quad u'_{1i}(s_2) + \chi_2 u_{1i}(s_2))_{i=1,2} = 0. \quad (12)$$

Here, the functions $u_{01}(s)$ and $u_{02}(s)$ are linearly independent solutions of the equation $Lu=0$, the function $u_{03}(s)$ is the particular solution of the equation $Lu+1=0$, and $u_{11}(s)$ and $u_{12}(s)$ are linearly independent solutions of the equation $Lu+r^{-2}u=0$. The values of χ_1 and χ_2 are determined by Eq. (10). Expressions for D_0 and D_1 can be also represented in the form

$$D_0 = A_0 \chi_1 \chi_2 + B_0 \chi_1 + C_0 \chi_2 + E_0, \quad (13)$$

$$D_1 = A_1 \chi_1 \chi_2 + B_1 \chi_1 + C_1 \chi_2 + E_1. \quad (14)$$

To determine if a given equilibrium state is stable, we first test the stability of the free surface to perturbations that leave the contact lines fixed. For this kind of perturbation, the boundary conditions (4) and (7) are replaced with the conditions $\varphi_0(s_1) = \varphi_0(s_2) = 0$ and $\varphi_1(s_1) = \varphi_1(s_2) = 0$, respectively. If a given free surface is unstable to these perturbations, the equilibrium state is also unstable.

Let us consider a free surface with fixed contact lines which is stable and compare the values χ_1 and χ_2 given by Eq. (10) with their critical values. The critical values χ_1^* and χ_2^* are determined from Eqs. (11) and (12) with χ_1 and χ_2 considered as independent variables. These equations are given by

$$D_0(\chi_1^*, \chi_2^*) = A_0 \chi_1^* \chi_2^* + B_0 \chi_1^* + C_0 \chi_2^* + E_0 = 0, \quad (15)$$

$$D_1(\chi_1^*, \chi_2^*) = A_1 \chi_1^* \chi_2^* + B_1 \chi_1^* + C_1 \chi_2^* + E_1 = 0. \quad (16)$$

The critical values χ_1^* and χ_2^* for axisymmetric perturbations belong to the right-and-upper branch of the hyperbola (15). This branch bounds the stability region \mathbf{S}_χ^0 in the χ_1 – χ_2 plane from the left and from below. For nonaxisymmetric perturbations, the stability region \mathbf{S}_χ^1 is bounded from below and from the left by the right-and-upper branch of the hyperbola (16). The doubly connected axisymmetric free surface is stable to arbitrary perturbations if the values of χ_1 and χ_2 given by Eq. (10) belong to the region of intersection of the regions \mathbf{S}_χ^0 and \mathbf{S}_χ^1 .

We use the above method to analyze the stability of a free surface in contact with a cylindrical wall and a flat endwall. For an annular surface that is in contact only with a cylindrical wall, this method may be considerably simplified (see Sec. III B).

III. RESULTS

A. A doubly connected free surface in contact with a cylindrical wall and a flat end

1. Preliminary analysis

We recast the equilibrium and perturbation equations in dimensionless form, using the cylinder radius, r_0 , to scale length. Then all the variables and functions in Eqs. (2)–(16) are replaced by their dimensionless analogs. In particular, s , r , z , and q are represented by their dimensionless counterparts S , R , Z , and Q , and ν , b and r_0 are replaced with V , B [see Eq. (1)] and 1, respectively. We set $S_1=0$ and place this point on an axial section of the cylinder's lateral wall. The points $S=S_{2i}$ ($i=1,2,\dots$) at which $\beta=\alpha$ (if they exist) are found (for fixed B , Q , and α) by numerically integrating

$$\begin{aligned} R'' &= -Z' \beta', & Z'' &= R' \beta', \\ \beta' &= -BZ + Q - \frac{Z'}{R} \quad \left(' = \frac{d}{dS} \right) \end{aligned} \quad (17)$$

together with the initial conditions

$$\begin{aligned} R(0) &= 1, & R'(0) &= -\sin \alpha, & Z(0) &= 0, \\ Z'(0) &= -\cos \alpha, & \beta(0) &= 270^\circ - \alpha. \end{aligned} \quad (18)$$

Provided that the functions $1-R(S)$ and $Z'(S)$ do not change sign from plus to minus as S increases from 0 to S_{2i} , each of the points $S=S_{2i}$ ($i=1,2,\dots$) may serve as the endpoint of the equilibrium profile on a given integral curve. This endpoint lies on a flat endwall with $Z=Z(S_{2i})$. In addition, we must find the endpoint S^* for the profile of a surface that is critical to perturbations with fixed contact lines. This profile can be determined in the same manner as the profile of a critical liquid bridge surface pinned to edges of circular disks.^{12,13} If $S_{2i} < S^*$ for a certain i , we then check the stability of the surface with a profile $0 \leq S \leq S_{2i}$ according to the method described in Sec. II. The numerical results presented in Secs. III A 2–III A 4 refer only to profiles with $S_{2i} < S^*$. Our calculations have shown that an integral curve may include no more than two equilibrium profiles that satisfy this condition.

For any Bond number and wetting angle values, an equilibrium surface with a profile $0 \leq S \leq S_{2i}$ ($S_{2i} < S^*$) is stable to nonaxisymmetric perturbations if $Q > -\cos \alpha$, and is unstable if $Q < -\cos \alpha$. For $Q = -\cos \alpha$, the curvature $\beta'(0) = 0$. Hence, $\chi_1 = 0$. It can be easily verified that in this case, the eigenvalue and the corresponding eigenfunction of the dimensionless analog to (6)–(7) are $\lambda = 0$ and $\varphi_1(S) = Z'(S)$. Furthermore, the values $\chi_1 = 0$ and $\chi_2 = -\beta'(S_{2i}) \cot \alpha$ belong to the right-and-upper branch of the hyperbola (16) so that the smallest eigenvalue $\lambda_{11} = 0$ corresponds to the eigenfunction $\varphi_1(S) = Z'(S)$. This means that an equilibrium surface with $Q = -\cos \alpha$ is neutrally stable to the most dangerous type of nonaxisymmetric perturbations for which the component normal to the axisymmetric equilibrium surface is proportional to $Z'(S) \cos \theta$. Inspection of the position of the point (χ_1, χ_2) shows that this point shifts into the \mathbf{S}_χ^1 region if Q becomes greater than $-\cos \alpha$, and shifts outside \mathbf{S}_χ^1 if $Q < -\cos \alpha$. For $0 \leq \alpha \leq 90^\circ$, an integral curve may only

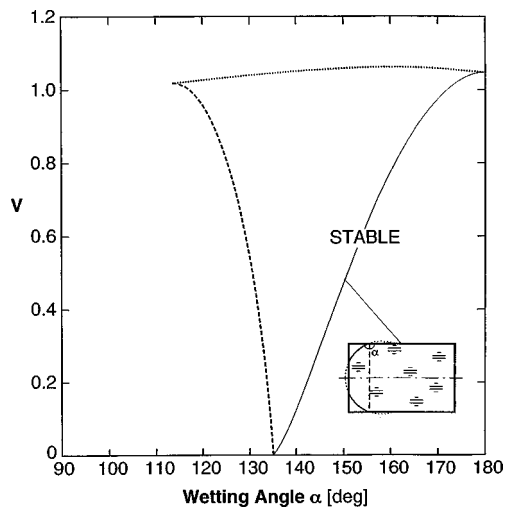


FIG. 2. Stability diagram for the zero gravity system ($B=0$) shown in Fig. 1. Dotted (dashed) line corresponds to states critical to axisymmetric (non-axisymmetric) perturbations. Solid line represents stable states with a free surface that conforms to a portion of a sphere.

contain an equilibrium profile when $Q < -\cos \alpha$. Hence, for any Bond number, the axisymmetric configuration under consideration is unstable if $0 \leq \alpha \leq 90^\circ$.

2. Zero gravity

As an illustration, let us first consider the stability conditions for $B=0$. The stability boundary in the α - V plane consists of two segments (Fig. 2). The upper segment corresponds to states that are critical to axisymmetric perturbations. The left-hand segment corresponds to states critical to nonaxisymmetric perturbations and originates from the point ($\alpha=135^\circ$, $V=0$). The solid line inside the stability region corresponds to the simplest configuration when the free surface is a piece of a sphere bounded by the cylinder wall and a flat endwall (see the inset in Fig. 2). The proof that such a surface is always stable is given in the Appendix.

For large wetting angles ($\alpha > 135^\circ$), there is only a maximum volume stability limit. For a fixed α , the solution to Eqs. (17)–(18) and, thus, a shape of an equilibrium profile depends on Q . The curve a in Fig. 3 is for $\alpha=145^\circ$ and illustrates a typical dependence of V on Q for $\alpha > 135^\circ$. Along this curve, the relative volume V tends to zero as $Q \rightarrow \infty$, and reaches the maximum value V_{\max} at $Q=1.504$. The point of maximum V corresponds to the state that is neutrally stable to axisymmetric perturbations ($\lambda_{01}=0$). If the integral curve of the problem (17)–(18) contains only one equilibrium profile, $0 \leq S \leq S_{21}$, the corresponding free surface is stable. There is an interval of Q values where the integral curve contains two profiles, $0 \leq S \leq S_{21}$ and $0 \leq S \leq S_{22}$, where $S_{22} > S_{21}$. The profile $0 \leq S \leq S_{21}$ corresponds to a stable surface, while the surface with a profile $0 \leq S \leq S_{22}$ may be stable ($Q < 1.504$), critical ($Q = 1.504$), or unstable to axisymmetric perturbations ($Q > 1.504$).

A set of equilibrium profiles for $\alpha=145^\circ$ is shown in Fig. 4(a). Each profile represents a portion $0 \leq S \leq S_{2i}$ ($i=1$ or 2) of the integral curve of the problem (17)–(18) that is displaced along the Z axis so that the endpoint S_{2i} lies on the

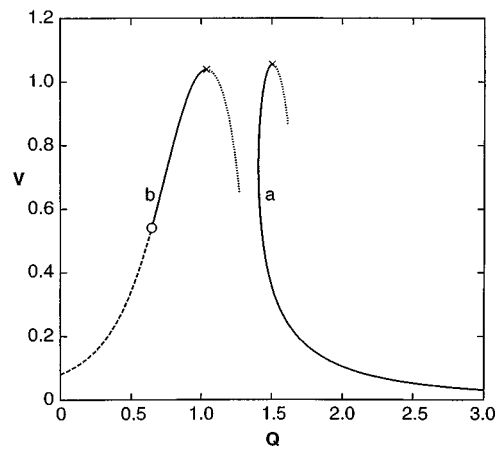


FIG. 3. Dependence of the relative gas volume, V , on the shape parameter, Q , for zero gravity configurations (Fig. 1) with $\alpha=145^\circ$ (curve a) and $\alpha=130^\circ$ (curve b). Solid lines correspond to stable states, and dotted (dashed) lines to states that are unstable to axisymmetric (nonaxisymmetric) perturbations. The open circle represents the point where $Q = -\cos \alpha$. A cross corresponds to the point of maximum V .

common flat endwall. We assumed that $Z=1$ at this end. Thus, for these profiles, $Z(0)$ is no longer equal to zero. Such a displacement is admissible for a cylindrical container. We use it hereafter to illustrate a set of profiles. The profiles a and b , terminate at $S=S_{22}$, while a closed circle corresponds to the point S_{21} . Profiles c and d represent portions $0 \leq S \leq S_{21}$ of the profiles b and a , respectively.

When $113.5^\circ < \alpha < 135^\circ$, there are both maximum and minimum volume stability limits. Stable states exist in the interval $V_{\min} < V < V_{\max}$. In this case, a typical dependence of V on Q takes the form of the curve b in Fig. 3. Here, in contrast to the case $\alpha > 135^\circ$, V tends to zero as $Q \rightarrow -\infty$. The value of Q corresponding to V_{\min} is $-\cos \alpha$. The equilibrium profiles a and c in Fig. 4(b) correspond to the maximum and minimum volume stability limits for $\alpha=130^\circ$. The minimum volume stability limit tends to zero as the wetting angle α tends to 135° (see Sec. III A 4).

Now let $R_2=R(S_2)$ be the dimensionless radius of a wetted spot on the flat end. Figure 5 shows the R_2 values for critical states. We see that the state becomes unstable to axisymmetric perturbations when, as this radius becomes small, the neck formed by the annular free surface becomes small. The loss of stability to axisymmetric perturbations results in breaking of the neck. After the neck breaks, the flat end will be entirely covered by the gas.

3. The effect of steady axial acceleration

Stability diagrams in the α - V plane for a set of Bond numbers are shown in Fig. 6. Figure 7 illustrates an influence of Bond numbers on the critical neck radius R_2 . Let us follow the evolution of the stability limits when changing the Bond number.

Positive Bond number. For all $B > 0$, the structure of the stability boundary is identical to that for zero gravity. The left most point of the stability boundary approaches the vertical line $\alpha=90^\circ$ as B increases. However, as pointed out in Sec. III A 1, it never reaches this line. The upper stability

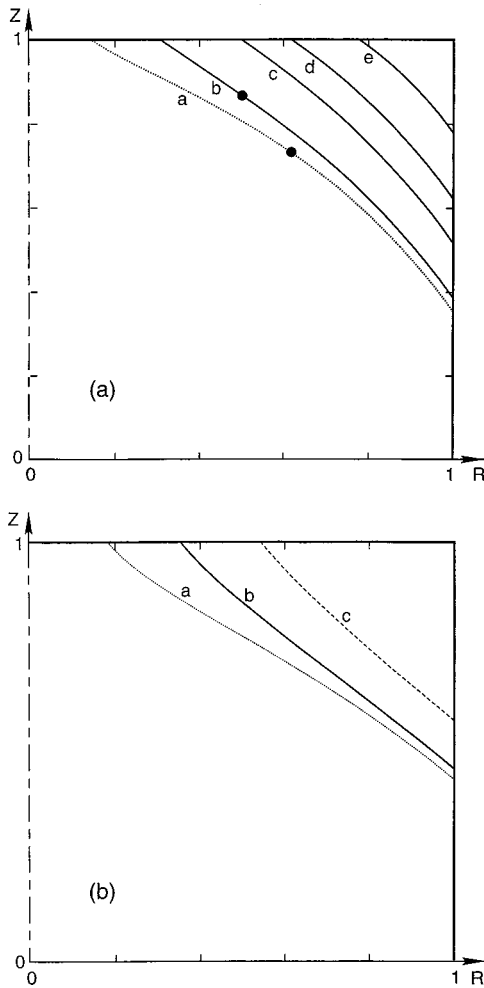


FIG. 4. Equilibrium surface profiles for zero gravity system shown in Fig. 1. (a) The case $\alpha=145^\circ$. Profiles *a*, *b*, *c*, *d*, and *e* correspond to Q values of 1.504, 1.42, 1.42, 1.504, and 1.9, respectively. (b) The case $\alpha=130^\circ$. Profiles *a*, *b*, and *c* correspond to $Q=1.038, 0.85$ and 0.643 . Solid lines correspond to stable surfaces, and dotted (dashed) lines to surfaces that are critical to axisymmetric (nonaxisymmetric) perturbations.

boundary moves down as B increases because the surface that bounds a given gas volume flattens and the neck radius R_2 decreases (see Fig. 8). In a qualitative sense, the dependence of V on Q has the same form as those described above (see Fig. 9).

Negative Bond number. The structure of the stability region and the nature of critical perturbations change when B passes through $B = -1.69$ and $B = -1.80$. For $-1.69 < B < 0$, the stability region is connected. The states on the boundary may be critical to nonaxisymmetric perturbations or axisymmetric perturbations. For $-1.69 < B < -0.84$, there are two segments of the boundary that correspond to critical nonaxisymmetric perturbations (see the stability boundary for $B = -1$ in Fig. 6). As the Bond number decreases and passes through the value -1.69 , the stability region breaks into two disconnected parts. The first part always exists for all Bond numbers less than -1.69 . For states belonging to the boundary of the first part, only nonaxisymmetric perturbations are critical. The second part exists only for Bond numbers between -1.69 and -1.80 . Its boundary is deter-

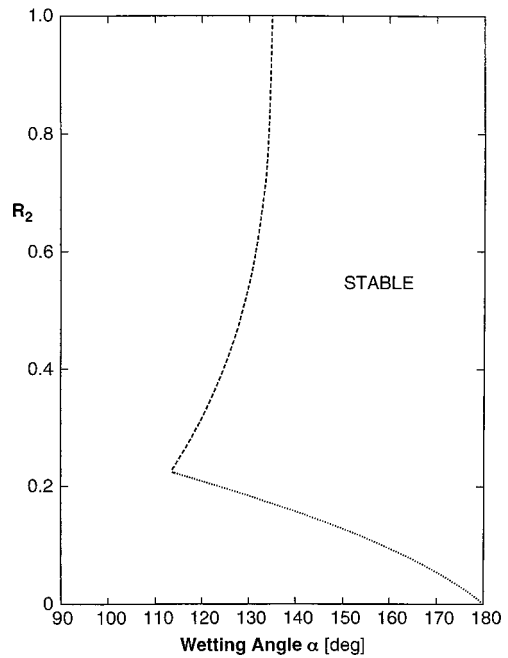


FIG. 5. Dependence of the radius R_2 of the contact line on a flat end on the wetting angle α for critical surfaces under zero gravity. The line styles are the same as in Fig. 2.

mined by the states that may be critical to nonaxisymmetric or axisymmetric perturbations.

The evolution of the stability region is clarified by Fig. 9. Here each $Q-V$ curve has been constructed for fixed values of α and B . Loss of stability to axisymmetric perturbations occurs at the point of maximum V . Loss of stability to nonaxisymmetric perturbations occurs at the point where $Q = -\cos \alpha$. When there are points with $Q < -\cos \alpha$ on the

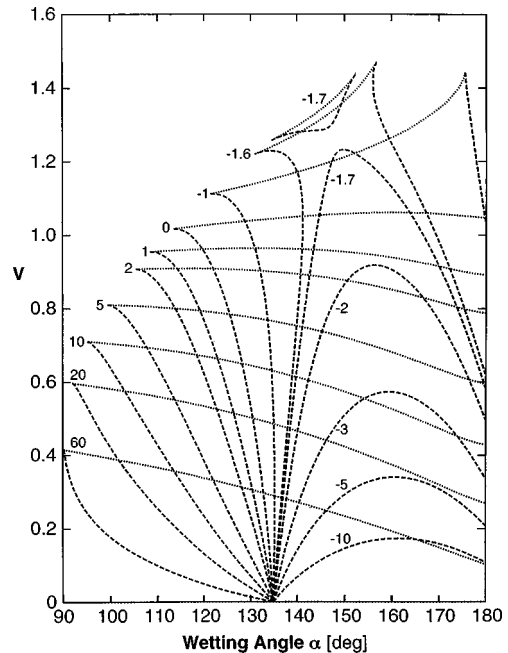


FIG. 6. Influence of the Bond number, B , on the stability limits for configurations shown in Fig. 1. Numbers on curves indicate the values of the Bond number. The line styles are the same as in Fig. 2.

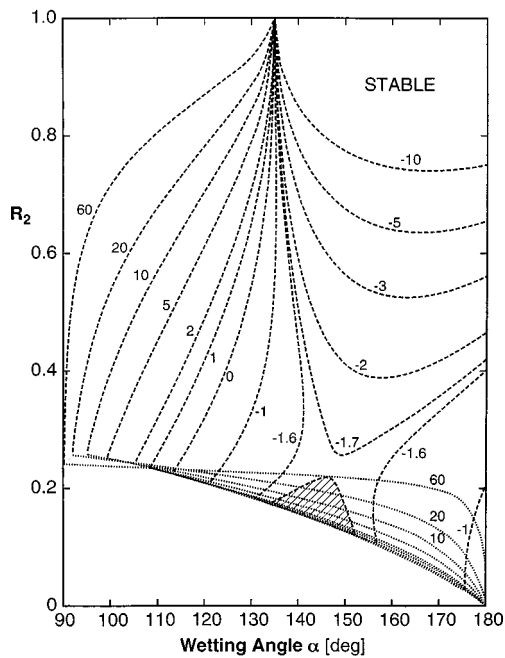


FIG. 7. Critical dimensional radius R_2 of the wetted portion of the flat endwall as a function of α . The corresponding Bond numbers are indicated on the curves. The line styles are the same as in Fig. 2. The shaded region is the disconnected part of the stability region for $B = -1.7$.

$Q-V$ curve for $\alpha > 135^\circ$ and when $Q > -\cos \alpha$ at the point of maximum V , two disconnected families of stable equilibrium states exist. This is illustrated by the curve for $\alpha = 145^\circ$ and $B = -1.7$. Equilibrium states are stable for $0 < V < 1.074$ ($0 \leq S \leq S_{21}, Q > 0.819 (= -\cos 145^\circ)$) and for $1.286 < V < V_{\max} = 1.341$ ($0 \leq S \leq S_{22}, 0.819 < Q < 0.866$), and are unstable for $1.074 < V < 1.286$ ($Q < 0.819$). Related equilibrium profiles are shown in Fig. 10 (a closed circle represents the point $S = S_{21}$ on the profile $0 \leq S \leq S_{22}$).

The loss of stability to axisymmetric perturbations results in the creation of an axisymmetric gas cavity that covers the cylinder base. From the result for the stability of

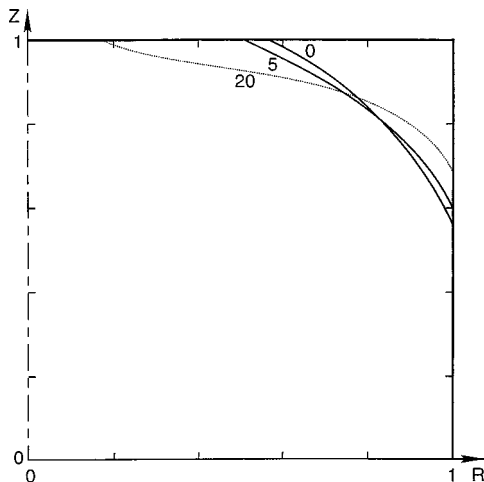


FIG. 8. Equilibrium surface profiles for $\alpha = 155^\circ$ and $V = 0.4$. Numbers on curves denote the values of B . Solid and dotted lines correspond to stable surfaces, and the surface critical to axisymmetric perturbations, respectively.

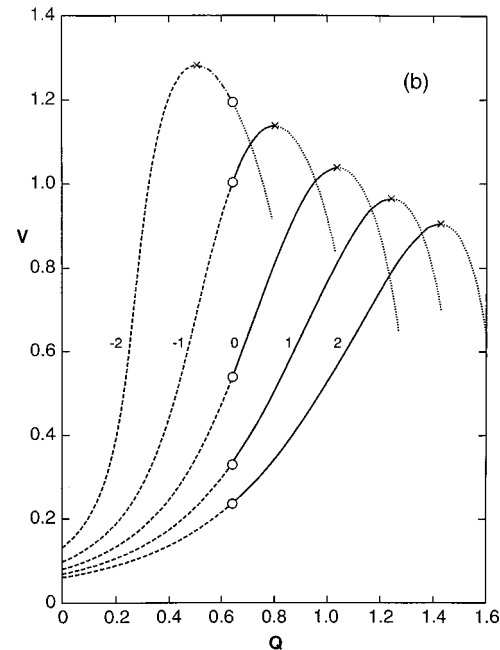
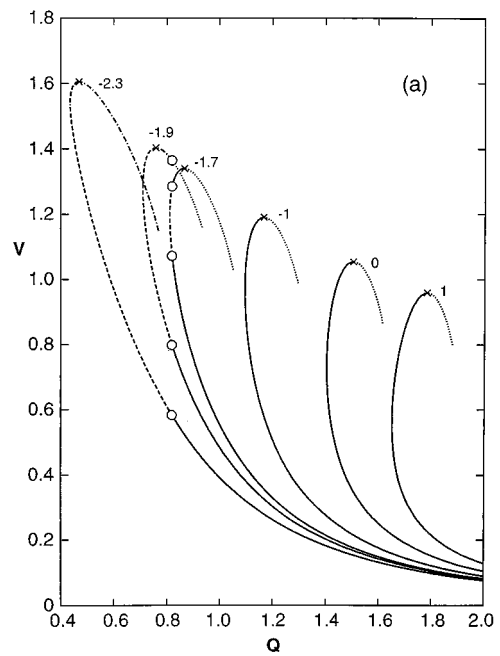


FIG. 9. The dependence of the relative gas volume, V , on the shape parameter, Q , at different Bond numbers, B , for wetting angle values $\alpha = 145^\circ$ (a) and $\alpha = 130^\circ$ (b). Numbers on curves indicate the values of B . Solid lines correspond to stable states, dotted (dashed) lines to states that are unstable to axisymmetric (nonaxisymmetric) perturbations, and dotted-dashed lines to states that are unstable to both axisymmetric and nonaxisymmetric perturbations. Open circles represent points with $Q = -\cos \alpha$. Crosses correspond to the points of maximum V .

simply connected axisymmetric surfaces in a cylinder,^{1,2} we can determine that this cavity is stable in equilibrium. It is believed that at large magnitudes of $B < 0$, loss of stability to nonaxisymmetric perturbations leads to a displacement of the gas cavity to the side of the container and detachment from the base.

4. The case $\alpha = 135^\circ$

For the system under consideration, the angle $\alpha = 135^\circ$ is special one. Equilibrium surfaces with a profile that is con-

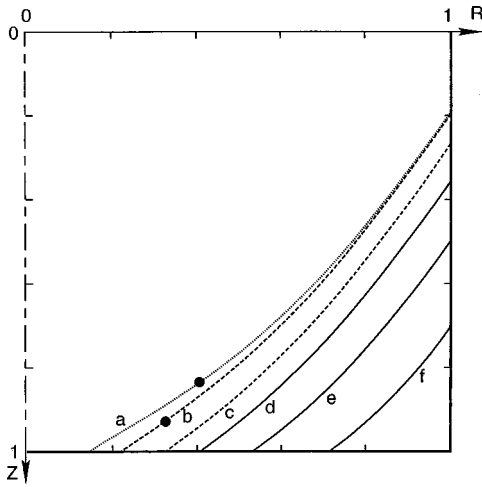


FIG. 10. Equilibrium surface profiles in the case $\alpha=145^\circ$ and $B=-1.7$. Profiles *a*, *b*, *c*, *d*, *e*, and *f* correspond, respectively, to the following values of Q (and V): 0.866 (1.341), 0.819 (1.286), 0.819 (1.074), 0.866 (0.860), 1.0 (0.557), and 1.4 (0.216). The line styles are the same as in Fig. 4.

vex toward the gas ($\beta'(S) > 0$ for $0 < S < S_2$) exist only for $\alpha > 135^\circ$, while surfaces with a profile concave toward the gas ($\beta'(S) < 0$) exist only for $\alpha < 135^\circ$.

If $\alpha = 135^\circ$, there is always an inflection point on the interior of the equilibrium profile. For $B \geq -\sqrt{2}/2$, such a profile may exist only if $Q > \sqrt{2}/2$, ($= -\cos 135^\circ = 0.707$), i.e., if the curvature at the initial point, $\beta'(0)$, is positive. The length S_2 of this profile (and thus the corresponding volume V) tends to zero as $Q \rightarrow \sqrt{2}/2 + 0$. For $B < -\sqrt{2}/2$, the equilibrium profile may also exist at $Q \leq \sqrt{2}/2$. If Q is close to, but less than $\sqrt{2}/2$, the integral curve of the system (17)–(18) includes two equilibrium profiles, $0 \leq S \leq S_{21}$ and $0 \leq S \leq S_{22}$. The length S_{21} of the smallest profile tends to zero as $Q \rightarrow \sqrt{2}/2 - 0$. The properties of equilibrium surfaces at $\alpha = 135^\circ$ that were described earlier are illustrated by the diagrams of equilibrium states in the $Q-V$ plane (Fig. 11).

According to Sec. III A 1, the $\alpha = 135^\circ$ surfaces are stable to nonaxisymmetric perturbations if $Q > \sqrt{2}/2$, and unstable to nonaxisymmetric perturbations if $Q < \sqrt{2}/2$. The segment enclosed by the point $Q = \sqrt{2}/2, V = 0$ and the point with $V = V_{\max}$ corresponds to surfaces that are stable to axisymmetric perturbations. The other surfaces are unstable. According to our calculations, the point with $V = V_{\max}$ has the value $Q > \sqrt{2}/2$ if $B \geq -1.71$.

Thus, for arbitrary perturbations, we can draw the following conclusions:

- (a) if $B \geq -\sqrt{2}/2$, stable states belong to the segment between the point $Q = \sqrt{2}/2, V = 0$ and the point with $V = V_{\max}(B)$;
- (b) if $-1.71 < B < -\sqrt{2}/2$, stable states correspond to the segment enclosed by the point $Q = \sqrt{2}/2, V > 0$ and the point with $V = V_{\max}(B)$;
- (c) if $B < -1.71$, stable states do not exist;
- (d) as $V \rightarrow 0$, equilibrium states approach the state critical to nonaxisymmetric perturbations; because of this, for any B , the stability boundary in the $\alpha-V$ plane (Fig. 6) emerges from the point $(135^\circ, 0)$.

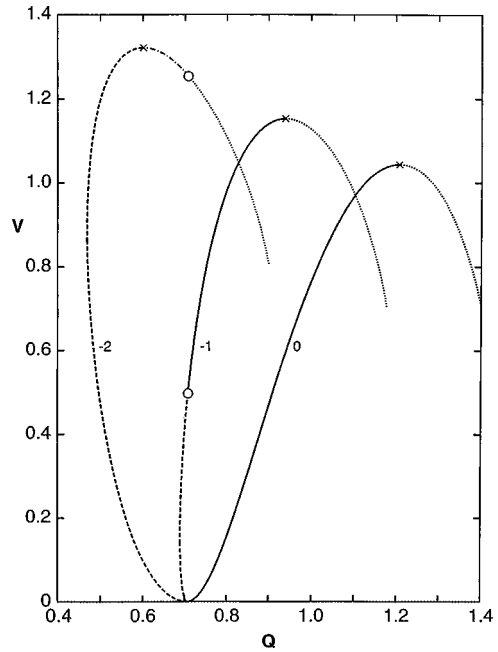


FIG. 11. Dependence of V on Q for equilibrium states with $\alpha=135^\circ$. Number on curves denote values of the Bond number. The line styles are the same as in Fig. 9. The states with $V = V_{\max}$ are denoted by \times , and the states with $Q = \sqrt{2}/2$ by open circles.

B. An annular free surface in contact with a cylindrical wall under zero gravity

The equilibrium configuration with both contact lines on the lateral wall of the cylinder (see the right-most inset in Fig. 12) may exist only under zero gravity conditions ($B = 0$). In this case, the free surface has an equatorial symmetry plane that is orthogonal to the cylinder's symmetry axis. The stability conditions for such a free surface with fixed contact lines have already been examined (see Refs. 2, 5, 8, 14, and 15). In the following, we consider surfaces that satisfy these conditions. In this subsection, we measure s from an equatorial point $s = 0$ of the equilibrium profile. That is, we assume

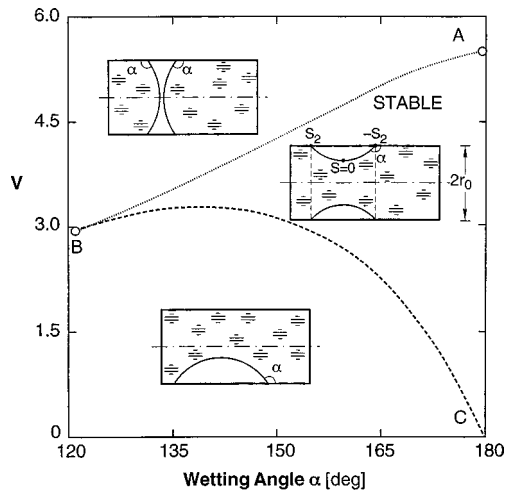


FIG. 12. Stability diagram for a zero gravity configuration with contact lines on the lateral wall of a cylinder.

that $-s_2 \leq s \leq s_2$ on the profile. The formulas in Sec. II are changed accordingly (taking $s = -s_2$ as the initial point). If we set

$$u_{01}(0) = 1, \quad u'_{01}(0) = 0, \quad u_{02}(0) = 0, \quad u'_{02}(0) = 1, \quad u_{03}(0) = 1, \quad u'_{03}(0) = 0, \tag{19}$$

$$u_{11}(0) = 1, \quad u'_{11}(0) = 0, \quad u_{12}(0) = 0, \quad u'_{12}(0) = 1, \tag{20}$$

the functions $u_{01}(s)$, $u_{03}(s)$, and $u_{11}(s)$ will be even while $u_{02}(s)$ and $u_{12}(s)$ will be odd. Considering that $\chi(-s_2) = \chi(s_2) = \chi$, we obtain from (11) and (12)

$$D_0 = 4[u'_{02}(s_2) + \chi u_{02}(s_2)] \left\{ [u'_{01}(s_2) + \chi u_{01}(s_2)] \times \int_0^{s_2} r u_{03} ds - [u'_{03}(s_2) + \chi u_{03}(s_2)] \int_0^{s_2} r u_{01} ds \right\}, \tag{21}$$

$$D_1 = 2[u'_{11}(s_2) + \chi u_{11}(s_2)][u'_{12}(s_2) + \chi u_{12}(s_2)]. \tag{21}$$

Since $u_{02}(s) = r'(s)$ and $u_{11}(s) = z'(s)$, the roots χ_{01}^* and χ_{02}^* of $D_0(\chi) = 0$ and the larger root χ_{11}^* of the equation $D_1(\chi) = 0$ have the form

$$\chi_{01}^* = - \frac{u'_{01}(s_2) \int_0^{s_2} r u_{03} ds - u'_{03}(s_2) \int_0^{s_2} r u_{01} ds}{u_{01}(s_2) \int_0^{s_2} r u_{03} ds - u_{03}(s_2) \int_0^{s_2} r u_{01} ds}, \tag{22}$$

$$\chi_{02}^* = \frac{z'(s_2)}{r'(s_2)} \beta'(s_2), \quad \chi_{11}^* = - \frac{r'(s_2)}{z'(s_2)} \beta'(s_2).$$

Thus, the stability condition reduces to the inequality

$$\chi > \max(\chi_{01}^*, \chi_{02}^*, \chi_{11}^*). \tag{23}$$

It can be easily verified that the value $\chi = -\beta'(s_2) \cot \alpha$ coincides with χ_{02}^* . This is because the equilibrium state under consideration allows arbitrary displacements along the axis of symmetry. A change in potential energy is zero under such displacements. Consequently, the problem (3)–(5) has the eigenvalue $\lambda = 0$, and the corresponding eigenfunction is $\varphi_0 = u_{02}(s) = r'(s)$. Such displacements along the axis of symmetry can be neglected when investigating the stability of the configuration's *shape*. The stability condition (23) then assumes the form

$$\chi (\equiv \chi_{02}^*) > \max(\chi_{01}^*, \chi_{11}^*). \tag{24}$$

An analysis of the inequality $\chi_{02}^* > \chi_{11}^*$ shows that only an unduloidal free surface with a profile that contains points of inflection $s = \pm s_{11}$ may be stable to nonaxisymmetric perturbations. Critical surfaces determining the segment *BC* of the stability boundary (Fig. 12) are unduloidal surfaces with profiles $-s_{11} \leq s \leq s_{11}$.

The boundary segment *BA* can be constructed upon testing the inequality $\chi_{02}^* > \chi_{01}^*$ numerically. The points of this segment correspond to unduloidal surfaces with profiles $-s_{01} \leq s \leq s_{01}$, such that $\chi_{02}^*(s_{01}) = \chi_{01}^*(s_{01})$ and $s_{01} > s_{11}$. The latter inequality is satisfied only for $\alpha > 121^\circ$.

For a given $121^\circ < \alpha < 180^\circ$, there exists a minimum volume stability limit V_{\min} (segment *BC*) and a maximum volume stability limit V_{\max} (segment *AB*). If $V > V_{\max}$, stability is lost to axisymmetric perturbations that are symmetric with

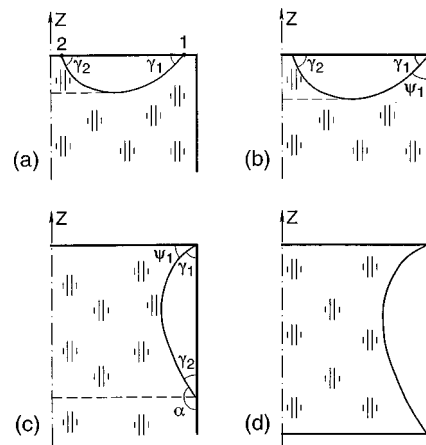


FIG. 13. Sketches of other doubly connected free surfaces in a cylindrical container. [Note that configurations (a) and (b) are nonequilibrium.]

respect to s , and the liquid breaks into two disconnected portions (see the inset in Fig. 12). If $V < V_{\min}$, loss of stability occurs to nonaxisymmetric perturbations, and the gas cavity will most probably shift to the side of the container.

C. Other doubly connected free surfaces

At first glance it seems that configuration with both contact lines on the endwall [Fig. 13(a)] remains to be examined. However, for the points 1 and 2 with the same value of z , the angle γ_2 is always greater than γ_1 under zero gravity and with axial steady acceleration (see Ref. 16 and also Refs. 2 and 4). Thus, if the smooth planar end of the cylinder is made of homogeneous material, an annular equilibrium surface with both contact lines on this end cannot exist.

When a container has an edge and both solid surfaces forming the edge are made from the same homogeneous material, a free surface in contact with this edge may be stable only if the region occupied by the liquid and the gas forms on the edge the dihedral angle that is greater than π .^{2,17} For a cylindrical container with a planar end, this angle is equal $\pi/2$. This means that any equilibrium configuration with a free surface contact line coinciding with the edge of a cylindrical container is unstable when the wetting angles along the cylindrical wall and the planar end are equal. The contact line will be displaced from the edge. Whether it moves to the endwall or the lateral wall depends on the relative positions of the liquid and gas and on the value of α . This is true for both simply connected and doubly connected free surfaces [Figs. 13(b)–13(d)].

Let us now assume that the wetting angles on the cylindrical wall and the planar end are different. First, we consider the case when one of contact lines coincides with the edge and the other lies on the endwall [Fig. 13(b)]. In analogy with Refs. 2 and 17, we find the following stability conditions with respect to perturbations that displace the contact line from the edge

$$\psi_1 \geq \alpha, \quad \gamma_1 \geq \pi - \alpha_1. \tag{25}$$

Here, α and α_1 are the wetting angles on the cylindrical wall and on the planar end, respectively, and ψ_1 and γ_1 are the

dihedral angles formed on the edge by the liquid and the gas [Fig. 13(b)]. On the other hand, since the free surface must satisfy Eqs. (2), we have $\gamma_1 < \gamma_2 = \pi - \alpha_1$ (see the first paragraph of this subsection). Thus, the second inequality in (25) cannot be fulfilled, and the configuration under consideration is always unstable.

If one of contact lines coincides with the edge and the other belongs to the cylindrical wall [Fig. 13(c)], we get the following inequalities instead of Eq. (25):

$$\psi_1 \geq \alpha_1, \quad \gamma_1 \geq \pi - \alpha. \quad (26)$$

From the expression obtained by the integrating the product of r and the second of equations (2) it follows that $\gamma_1 > \gamma_2$ for $B > 0$, $\gamma_1 = \gamma_2$ for zero gravity, and $\gamma_1 < \gamma_2$ for $B < 0$. Since $\gamma_2 = \pi - \alpha$, a stable equilibrium is not possible for the latter case and may exist only in the first two cases if $\alpha > \alpha_1 + \pi/2$. To make a complete conclusion on the stability of the configuration for $B > 0$ and $B = 0$, arbitrary perturbations must be accounted for.

For the configuration with contact lines located on the edges of the cylinder's two flat endwalls [Fig. 13(d)], the stability to arbitrary perturbations for the case of different wetting angles α , α_1 and α_2 on the lateral wall and the ends has been analyzed in Ref. 18.

IV. CONCLUSIONS

The results obtained here represent the completion of a study of the shape and stability of connected axisymmetric equilibrium surfaces in a cylindrical container under zero gravity and a steady acceleration directed along the cylinder's axis. If the wetting angle is constant on the entire cylindrical container, the possible axisymmetric annular configurations, except for free surfaces with contact lines on each (materially different) flat endwall, are the configurations shown in Figs. 1 and 12. The shape and stability of the above configurations depend on the relative volume of an annular region bounded by the free surface and the interior surface of the container. For these configurations, a scale volume is not the cylinder's volume, but is equal (or proportional) to the cube of the cylinder radius.

The second parameter governing the stability of equilibrium is the wetting angle. We have shown that, for an annular region occupied by a gas and for wetting angles less than 121° , a stable equilibrium cannot exist for the system shown in Fig. 12. The same is true for the system shown in Fig. 1 if $\alpha \leq 90^\circ$. In addition, for this system, the stability conditions when $\alpha < 135^\circ$ and $\alpha > 135^\circ$ are quite different.

Finally, the equilibrium and stability of the system shown in Fig. 1 depend on the Bond number. Stability is not possible for $\alpha \leq 135^\circ$ if $B < -1.71$, but is possible for $135^\circ < \alpha < 180^\circ$ at any Bond number.

The behavior of the stability limit has been analyzed in detail for arbitrary constant volume perturbations. We can definitely predict the consequences when stability is lost to axisymmetric perturbations. What happens following loss of stability to nonaxisymmetric perturbations remains an open question. In particular, when, for fixed α and B , the stability region consists of two disconnected parts (Fig. 6). It would

be interesting to understand the transition between the two parts upon variation of the gas relative volume. In this respect, a study of the related bifurcation problem would provide useful information (see for example, the analysis described in Ref. 15 for liquid bridges with fixed contact lines).

ACKNOWLEDGMENTS

This work was supported by the National Aeronautics and Space Administration through Grant No. NAG3-2160.

APPENDIX: STABILITY OF A FREE SURFACE CONFORMING TO A PIECE OF SPHERE BOUNDED BY A CYLINDRICAL WALL AND A FLAT ENDWALL

The first system considered is shown in Fig. 1. The simplest configuration of this system is when a free surface with $B = 0$ is a piece of a sphere. This configuration is found to exist only for $\alpha > 135^\circ$. The corresponding stability problem can be solved analytically. A surface that conforms to a portion of sphere is always stable to perturbations that leave the contact lines fixed.² It can easily be verified that the following equations are valid

$$r = -\bar{R} \cos x, \quad x = \frac{s}{\bar{R}} - \alpha, \quad s_1 = 0, \quad (A1)$$

$$s_2 = \bar{R} \left(2\alpha - \frac{3}{2}\pi \right), \quad a = -\frac{2}{\bar{R}^2},$$

$$u_{01} = \sin x, \quad u_{02} = -1 + \frac{1}{2} \sin x \ln \frac{1 + \sin x}{1 - \sin x},$$

$$u_{03} = \frac{1}{2} \bar{R}^2, \quad u_{11} = \cos x, \quad (A2)$$

$$u_{12} = \tan x + \frac{1}{2} \cos x \ln \frac{1 + \sin x}{1 - \sin x},$$

where $\bar{R} = -r_0 \sec \alpha$ is the sphere radius. To within common factors, the coefficients of Eqs. (13) and (14) assume the form

$$A_0 = \bar{R}^2 (\sin \alpha + \cos \alpha) \left\{ \sin \alpha + \cos \alpha + (1 + \sin \alpha \cos \alpha) \ln \left[\tan \left(\frac{\alpha}{2} - \frac{\pi}{4} \right) \tan \frac{\alpha}{2} \right] \right\}, \quad (A3)$$

$$B_0 = \bar{R} \left\{ \cos^2 \alpha - 2 \sin^2 \alpha - \sin^2 \alpha \tan \alpha + \cos \alpha (\sin^2 \alpha + 2 \cos^2 \alpha + 2 \sin \alpha \cos \alpha) \ln \left[\tan \left(\frac{\alpha}{2} - \frac{\pi}{4} \right) \tan \frac{\alpha}{2} \right] \right\}, \quad (A4)$$

$$C_0 = -\bar{R} \left\{ \sin^2 \alpha - 2 \cos^2 \alpha - \cos^2 \alpha \cot \alpha + \sin \alpha (\cos^2 \alpha + 2 \sin^2 \alpha + 2 \sin \alpha \cos \alpha) \ln \left[\tan \left(\frac{\alpha}{2} - \frac{\pi}{4} \right) \tan \frac{\alpha}{2} \right] \right\}, \quad (A5)$$

$$E_0 = 2(\sin \alpha + \cos \alpha) \left\{ \sin \alpha \tan \alpha + \cos \alpha \cot \alpha - \sin \alpha \cos \alpha \ln \left[\tan \left(\frac{\alpha}{2} - \frac{\pi}{4} \right) \tan \frac{\alpha}{2} \right] \right\}, \quad (A6)$$

$$A_1 = \bar{R}^2 \left\{ \sin \alpha \tan \alpha + \cos \alpha \cot \alpha - \sin \alpha \cos \alpha \ln \left[\tan \left(\frac{\alpha}{2} - \frac{\pi}{4} \right) \tan \frac{\alpha}{2} \right] \right\}, \quad (A7)$$

$$B_1 = \bar{R} \sin \alpha \left\{ 1 + \sec^2 \alpha - \cot \alpha + \sin \alpha \ln \left[\tan \left(\frac{\alpha}{2} - \frac{\pi}{4} \right) \tan \frac{\alpha}{2} \right] \right\}, \quad (A8)$$

$$C_1 = -\bar{R} \cos \alpha \left\{ 1 + \csc^2 \alpha - \tan \alpha + \cos \alpha \ln \left[\tan \left(\frac{\alpha}{2} - \frac{\pi}{4} \right) \tan \frac{\alpha}{2} \right] \right\}, \quad (A9)$$

$$E_1 = \sin \alpha + \cos \alpha + \sec \alpha + \csc \alpha + \sin \alpha \cos \alpha \ln \left[\tan \left(\frac{\alpha}{2} - \frac{\pi}{4} \right) \tan \frac{\alpha}{2} \right]. \quad (A10)$$

For the case being considered, $\chi_1 = \chi_2 = \chi = -\bar{R}^{-1} \cot \alpha$. Substituting this expression and Eqs. (A3)–(A10) into (13) and (14), we obtain

$$D_0 = 1 - 2 \cot^2 \alpha - \cot \alpha + \frac{2(\sin \alpha + \cos \alpha)}{\sin^2 \alpha \cos \alpha} + \frac{\cos^3 \alpha}{\sin^2 \alpha} \ln \left[\tan \left(\frac{\alpha}{2} - \frac{\pi}{4} \right) \tan \frac{\alpha}{2} \right], \quad (A11)$$

$$D_1 = 2 \sin^{-3} \alpha.$$

Neither D_0 nor D_1 change their sign in the interval $135^\circ < \alpha < 180^\circ$. This means that there is no critical state for a configuration corresponding to a portion of a sphere. All such configurations are either stable or unstable. To determine whether the configuration is unstable or stable, we compare, for any α on the interval $135^\circ < \alpha < 180^\circ$, the χ with the largest root of the equations $D_0(\chi^*) = 0$ and $D_1(\chi^*) = 0$ that

follow from Eqs. (15) and (16) after the substitution of Eqs. (A3)–(A10) and $\chi_1^* = \chi_2^* = \chi^*$. The result of the comparison is that χ is larger than the largest root and, thus, a surface that conforms to a portion of a sphere is always stable.

¹A. D. Tyuptsov, "Hydrostatics in weak force fields. Stability of the equilibrium shapes of a liquid surface," *Izv. Akad. Nauk SSSR, Mekh. Zhidk. Gaza* No. 2, 78 (1966) (in Russian).
²A. D. Myshkis, V. G. Babskii, N. D. Kopachevskii, L. A. Slobozhanin, and A. D. Tyuptsov, *Low-Gravity Fluid Mechanics* (Springer-Verlag, Berlin, 1987).
³D. H. Michael, "Meniscus stability," *Annu. Rev. Fluid Mech.* **13**, 189 (1981).
⁴R. Finn, *Equilibrium Capillary Surfaces* (Springer-Verlag, New York, 1986).
⁵L. A. Slobozhanin, "Problems of stability of an equilibrium liquid encountered in space technology research," in *Fluid Mechanics and Heat/and Mass Transfer Under Zero Gravity* (Nauka, Moscow, 1982), p. 9 (in Russian).
⁶I. D. Borisov, "Stability of the equilibrium of a capillary fluid in a horizontal slit," *Izv. Akad. Nauk SSSR, Mekh. Zhidk. Gaza* No. 5, 174 (1983) (in Russian); English Translation: *Fluid Dyn. (USSR)* **18**, 806 (1983).
⁷T. I. Vogel, "Stability of a liquid drop trapped between two parallel planes," *SIAM J. Appl. Math.* **49**, 516 (1987).
⁸L. A. Slobozhanin, "Some problems of stability of zero-g liquid bridges," in *Hydromechanics and Heat/Mass Transfer in Microgravity* (Gordon and Breach Sci. Publ., New York, 1992), p. 185.
⁹D. Langbein, "Stability of liquid bridges between parallel plates," *Microgravity Sci. Technol.* **V/1**, 2 (1992).
¹⁰P. Concus and R. Finn, "Discontinuous behavior of liquids between parallel and tilted plates," *Phys. Fluids* **10**, 39 (1998).
¹¹T. Duffar and J. Abadie, "Wetting of InSb melts on crucibles in weightlessness—Results of the TEXUS 32/TEM 01-4 experiment," *Microgravity Sci. Technol.* **IX/1**, 35, (1996).
¹²L. A. Slobozhanin and J. M. Perales, "Stability of liquid bridges between equal disks in an axial gravity field," *Phys. Fluids A* **5**, 1305 (1993).
¹³L. A. Slobozhanin, M. Gomez, and J. M. Perales, "Stability of liquid bridges between unequal disks under zero-gravity conditions," *Microgravity Sci. Technol.* **VIII/1**, 23 (1995).
¹⁴R. D. Gillette and D. C. Dyson, "Stability of fluid interfaces of revolution between equal solid circular plates," *Chem. Eng. J.* **2**, 44 (1971).
¹⁵L. A. Slobozhanin, J. I. D. Alexander, and A. H. Resnick, "Bifurcation of the equilibrium states of a weightless liquid bridge," *Phys. Fluids* **9**, 1893 (1997).
¹⁶H. C. Wente, "The symmetry of sessile and pendent drops," *Pac. J. Math.* **88**, 387 (1980).
¹⁷L. A. Slobozhanin and A. D. Tyuptsov, "Stable equilibrium of the surface of a capillary liquid in contact with the edge of a solid," *Izv. Akad. Nauk SSSR, Mekh. Zhidk. Gaza* No. 1, 3 (1974) (in Russian); English Translation: *Fluid Dyn. (USSR)* **9**, 1 (1974).
¹⁸L. A. Slobozhanin, J. I. D. Alexander, and V. V. Rakov, "Contactless directional crystallization," *J. Cryst. Growth* (in press).